

## DAY TO DAY VARIATION OF MEAN TURBULENCE FEATURES IN A MONSOON ABL DURING PASSAGE OF A DEPRESSION

B ROY\*, U K DE\*, B PAL† AND B CHAKRAVARTY†

*\*Physics Department, Jadavpur University 2nd Campus, Block LB,  
Plot-8, Sector III, Salt Lake, Calcutta 700 091, India*

*†Department of Physics & Meteorology,  
Indian Institute of Technology, Kharagpur, 721 302, India*

*(Received 07 February 1995; Revised 25 May 1995;  
Accepted 26 July 1995)*

Doppler acoustic sounder is used to obtain wind information over inversion depth at 0530 hours each day between August 28 and September 08, 1990. The span includes a period before and after the passage of a depression in the vicinity of Station-Kharagpur. Data are used to calculate various mean turbulence quantities at the time of sounding and an analysis of the quantities in relation to pressure trough orientation marked by the passage of a depression is made. Lastly, the impact of such a depression on inversion and mixing depth is brought out taking their time-series.

**Key Words:** MONTBLEX; Sodar; Radar; Depression; Microscale; Turbulence; Inversion; Mixing; Trough

### Introduction

Understanding and parameterising of the mean turbulent process at inversion top is important to obtain analytical solutions that define motion in turbulent Atmospheric Boundary Layer (ABL) resulting into a mixed layer under stable ABL conditions. This cannot be achieved without taking into account of the small scales of motion.

In fact, the smallest scales of motion essentially result in viscous dissipation and hence mixing. Conservation of momentum must resolve these dissipative eddies<sup>1</sup> whose length scales are comparable with the scale of smallest fluid motion, called the Kolmogorov microscale<sup>2</sup>.

Static stability and wind shear effect mixing of momentum and refractive index in the same manner<sup>3</sup>. Acoustic sounders are able to sense the properties of mean turbulence quantities in ABL<sup>4</sup> but, with limited accuracy<sup>5</sup>. Hill<sup>6</sup> points out the importance of knowledge about the Kolmogorov microscale of turbulence, and mentions about its applications to ascertain a critical wavelength for radio detection and ranging (radar) performance.

These mean turbulence quantities in ABL were needed to be observed under monsoon conditions, hence we report few observed behaviour of such quantities occurring at the inversion-top while the ABL is under early morning fumigation period (around 0530 hours, Local Standard Time, LST). Under such a condition it is believed that mixed layer below the ABL top (inversion

height,  $Z_i$ ) is affected mainly by the entrainment of air from aloft and the wind shear at inversion depth<sup>7</sup>.

A comparative study of the nature of variation of dissipation length scale and Kolmogorov microscale is made. This is done using few empirical expressions that are reported earlier. In doing so a Doppler Sonic Detection and Ranging (sodar) system (Aerovironment make, model V-2000) data-set is made use of, for a disturbed and an undisturbed day.

We also report in this paper some of the characteristics of variation of wind-field turbulence estimators and an analysis is made on collective informations obtained on the variation of eddy size and turbulence mixing length by calculating few scales of mean turbulence. Observations pertain to the mid-monsoon phase (August 28-September 08, 1990).

The mean turbulence quantities and their nature of variation at inversion depth on a day-to-day basis are discussed in the light of coincident synoptic features during the period of observations. Lastly, the time series of inversion depth (in metres) as well as the mixing depth (in metres) is presented for the above-mentioned period, and the impact of land depression on its day-to-day variation pattern is also discussed.

### **Experiment and Sodar Data**

In monsoon, ABL vertical velocity and related parameters are responsible for organisation of cumulus convection. Land-locked ABL processes in the monsoon trough region present a marked variation with respect to: (a) deep moist convection in the eastern end of the trough over north Bay of Bengal and adjoining areas ( $85^{\circ}$ - $90^{\circ}$ E); and (b) alternation of deep moist/unsaturated processes along  $75$ - $85^{\circ}$ E within the trough over parts of eastern India. During the monsoon season of 1990 a widespread meteorological experiment was undertaken between May 16 and September 10, 1990. The experiment was acronymed MONTBLEX (Monsoon Trough Boundary Layer Experiment). The details of the experiment have already been published<sup>8,9</sup>. Such an experiment was unique in a tropical region like India whence the monsoon trough persists for about four months. Our study is confined to station Kharagpur, ( $22^{\circ}18'N$ ,  $87^{\circ}12'E$ ), a near-sea-coast station situated about 80 km away from the Bay of Bengal shoreline.

A depression was formed as a remnant of a Typhoon termed 'Becky' that emerged as low in the NE Bay of Bengal after crossing the Arakan coast (see tracks in Fig. 1). This depression had a track that followed dissipation stage in the period between August 28 and September 09, 1990. It further concentrated on to a land depression during its W-N-W track and maintained its intensity for about 24 hours. Life-span was for about 9 to 10 days and it caused fairly well distributed rainfall<sup>10</sup>.

It was found that the pressure trough axis was slightly varying over station Kharagpur during the period between September 5 and 8 (c.f Fig. 2). This is also evident from the erratic pressure tendency situation that occurred during the entire period of our observation. However, because of the absence of any elevated layer formation we deduce that there was no considerable frontal ac-

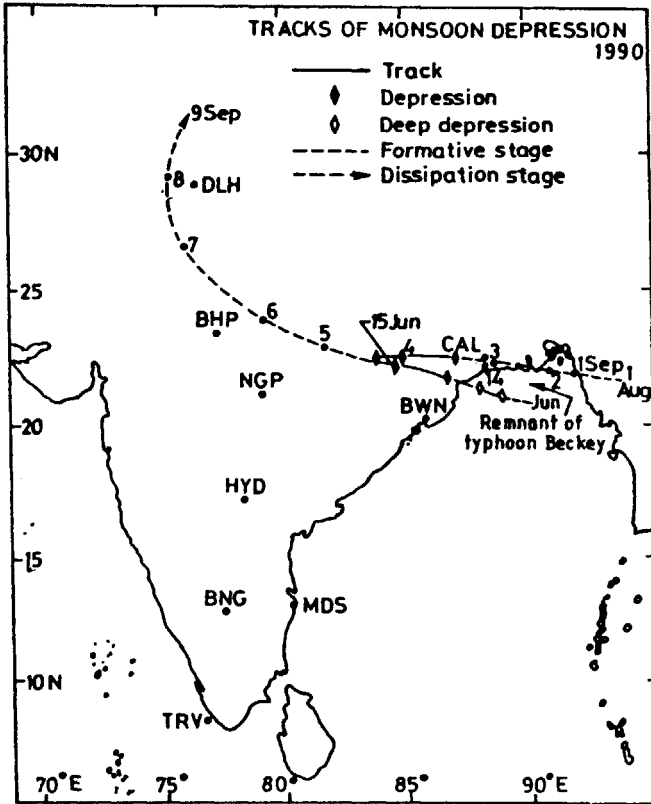


Fig 1 Tracks of monsoon-1990 depression<sup>10</sup>

tivity during the moist diabatic convection mechanism active during the morning hours of sounding.

Details about the site of the experiment and general meteorological conditions prevailing over the site during the experimental period have appeared in few published research papers<sup>11,12</sup>.

A 3-axis Doppler sodar with a 1.2 metre dish diameter and 1497 Hz frequency of transmission was deployed at station Kharagpur. The sodar system was optimised and then installed at the site by the Indian Institute of Tropical Meteorology (Pune). The details of the sounder employed may be found in published papers<sup>12-15</sup>. Within a distance of about 200 yards from the sodar site, a 30 m high micrometeorological tower was erected to measure slow-response (1 sample per second) data of wind, temperature and humidity at 6 levels. Sensors were mounted on the upwind side of the tower. Most of the background noise at sodar site and at nearby environment was mainly due to railway traffic, low flying small aircrafts, birds and insects. The Doppler sodar registered wind components i.e.,  $\bar{u}$  (EW),  $\bar{v}$  (NS),  $\bar{w}$  (vertical) and its standard deviation

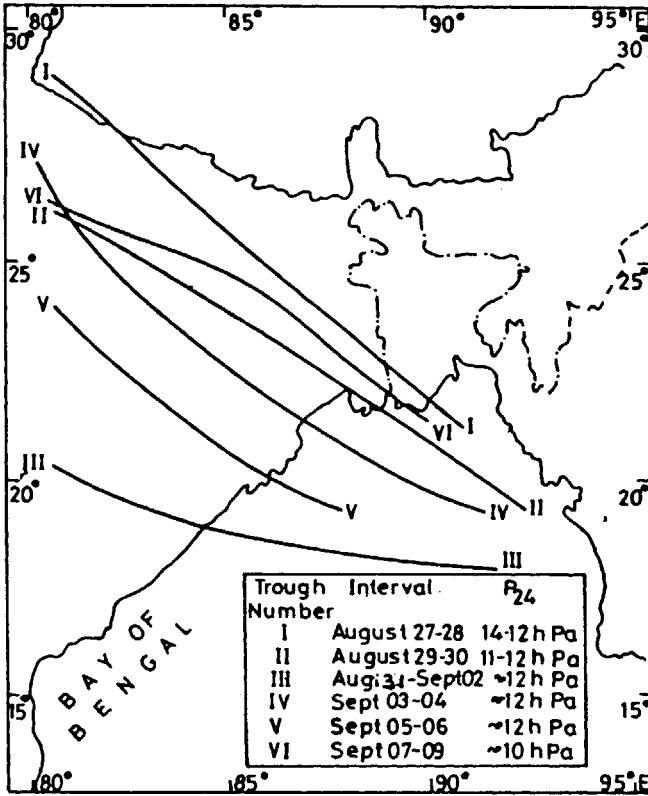


Fig 2 Map of the eastern part of India showing orientations of pressure trough axes with an inset describing details of dates and pressure tendency

in m/s ( $\sigma_w$ ), backscatter intensity, Inversion depth ( $Z_i$ ) and mixing layer depth (in metres). These data were either averages of 30 or 60 minutes.

Explanations on Doppler sodar measurement of  $u$ ,  $v$  and  $w$  components of wind in the ABL are well made in many literatures e.g., in Mingyu *et al.*<sup>13</sup>  $Z_i$  is ascertained from the echo-intensity profile. The backscatter intensities are proportional to the high frequency temperature fluctuation at those ranges<sup>14</sup>. The depth at which the backscatter intensity increases by more than or about 5 units is taken to be the inversion depth. Whereas the mixing depth is ascertained from the depth of a first minimum in the similar profile (cf. Fig. 3 of ref. 14).

### Turbulence Quantities

#### Cross-Wind Standard Deviation ( $\sigma_v$ )

This represents variation of wind velocity perpendicular to the mean wind direction and is a suitable estimator of variability of horizontal wind direction which persists, and is independent of changes in wind speed. Downwind stand-

ard deviation ( $\sigma_u$ ) represent variation in wind velocity along the mean wind direction and is a measure of variability in horizontal wind speed without regard to changes in wind direction.  $\sigma_v$  and wind direction standard deviation ( $\sigma_\phi$ ) are related as,

$$\sigma_\phi = \text{Tan}^{-1} \left( \frac{\sigma_v}{\bar{U}} \right), \quad \dots (1)$$

where

$$\phi = \text{Tan}^{-1} \left( \frac{\bar{u}}{\bar{v}} \right). \quad \dots (2)$$

$\sigma_v$  and  $\sigma_u$  may be mathematically written following Aerovironment Inc.<sup>15</sup>—

$$\sigma_v = \left( \frac{\bar{u}^2 (2\sigma_N)^2 - \bar{v}^2 (2\sigma_E)^2}{(\bar{u}\bar{v})} \right)^{0.5} \quad \dots (3)$$

and

$$\sigma_u = \left( \frac{\bar{u}^2 \sigma_v^2 - \bar{v}^2 (2\sigma_N)^2}{(\bar{u}\bar{v})} \right)^{0.5}. \quad \dots (4)$$

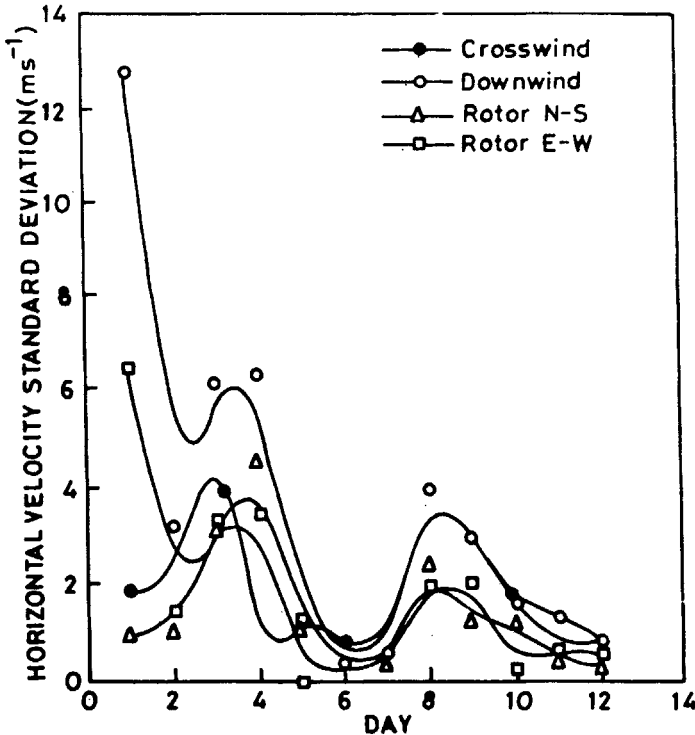


Fig 3 Day to day variation of horizontal wind velocity standard deviations (m/s) at  $Z_i$  (sodar measured)

$\sigma_N$  and  $\sigma_E$  are accurately measured variations in wind velocities occurring in the antenna orientation axes respectively. The factor 2 comes due to the component resolution arising due to the antenna tilt of 30 degrees from the ground level. Fig. 3 shows variation of these quantities (day-wise) at  $Z_i$ .

### Turbulence Intensity (I)

In order to measure magnitude of the spread in horizontal wind speed from its mean, we use turbulence intensity ( $I$ ) as per definition of Stull<sup>16</sup>

$$I = (\sigma_u / \bar{U}), \quad \dots (5)$$

where, in our case, most of the turbulence intensity at  $Z_i$  should be contributed due to mechanical processes only. It is now noted that intensity is considerably high even during 0530 hours at inversion depths of each day (see Fig. 4) while ground based inversion is maintained between 90 and 210 metres, AGL. No elevated inversion occurred on any of these days except on September 7 morning hours. It is also found that the intensity never exceeds 0.5, conditionally maintaining the Taylor's explanation (as mentioned in ref. 17).

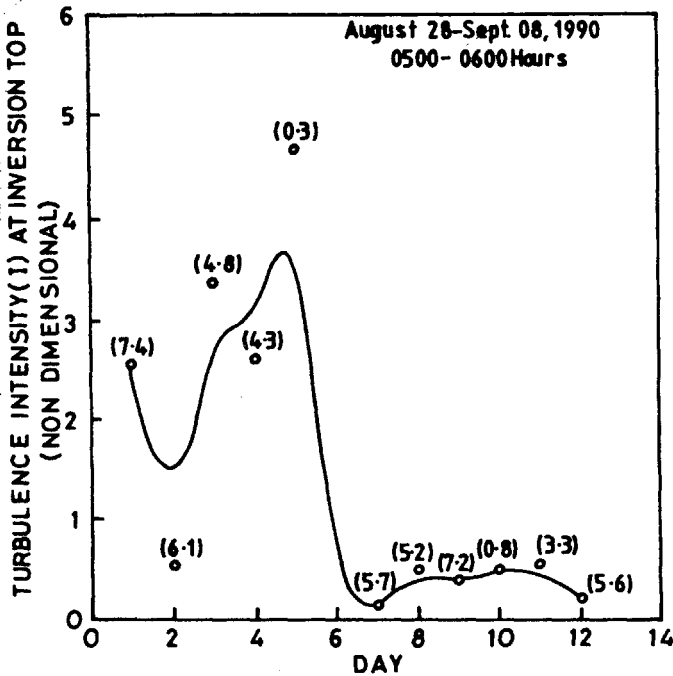


Fig 4 Day to day variation of mean turbulence intensity. Absolute magnitudes of  $U$  at  $Z_i$  are also shown in parentheses

### Turbulence Related Variables

Variation in magnitude of few turbulence quantities at inversion height on each day of observation is studied for the periods when the ABL is under morning fumigation condition. Mean Kinetic Energy per unit mass (MKE/ $m$ ), Kolmog-

orov microscale ( $\eta_k$ ), turbulence intensity ( $I$ ), dissipation length scale ( $d_l$ ), dissipation rate of turbulent kinetic energy ( $\epsilon$ ) are computed from Doppler sodar measured wind data and related parameters. A day to day variation of these quantities is evident from the plots in the following sections. Table I gives few Doppler sodar derived magnitudes of ABL parameters (day-wise).

**MKE/m**

This energy arises out of interactions between the mean flow of wind and turbulence components that are produced mechanically in the ABL. MKE/m is actually the amount of energy available for conversion to turbulence and can be written as

$$MKE/m = 0.5 (\bar{u}^2 + \bar{v}^2 + \bar{w}^2). \quad \dots (6)$$

Fig. 5 reveals that this fraction of energy that is ideally converted to the shear flow, vary almost inversely with turbulence intensity ( $I$ ) at  $Z_i$  (cf. Figs 4 and 5).

**Table I**

*Some ABL parameters with magnitudes occurring over the inversion depth as observed by the Doppler sodar during the observation period (Aug. 28-Sept. 08, 1990)*

Date	Day	Inversion height (m)	Mixing height (m)	Cloud (octa)	$\Delta \bar{U}$ (m/s)	$\Delta \phi$ (deg)	$\sigma_\phi$ (deg)	$\phi$ (deg)
28/8	1	600	240	2/8	6.5	183	0	344
29/8	2	180	60	8/8	2.3	104	14	118
30/8	3	180	120	3/8	1.5	178	16	106
31/8	4	120	60	3/8	0.1	45	7	89
01/9	5	180	150	5/8	0.4	351	5	307
02/9	6	150	60	7/8	1.0	225	8	257
03/9	7	120	90	7/8	0.9	343	7	289
04/9	8	570	450	6/8	1.6	326	38	302
05/9	9	510	450	6/8	6.8	333	0	137
06/9	10	120	60	2/8	0.6	189	28	138
07/9	11	270	150	4/8	0.4	18	6	244
08/9	12	210	120	4/8	0.7	251	9	215

**Kolmogorov Microscale**

Kolmogorov microscale is denoted by  $\eta_k$  and is an absolute indicator of the viscous eddy size. In this scale-range it is assumed that the inertial sub-range spectrum has a dissipative range of eddies scaling in size with  $\eta_k$ , also known as momentum diffusivity<sup>18</sup>. This may be mathematically written as

$$\eta_k = \left( \frac{\nu^3}{\epsilon} \right)^{1/4} \quad \dots (7)$$

where  $\nu$  is the kinematic viscosity of air.  $\epsilon$  is calculated in terms of velocity structure parameter ( $C_v^2$ ) from the limiting relation derived from a mixed layer

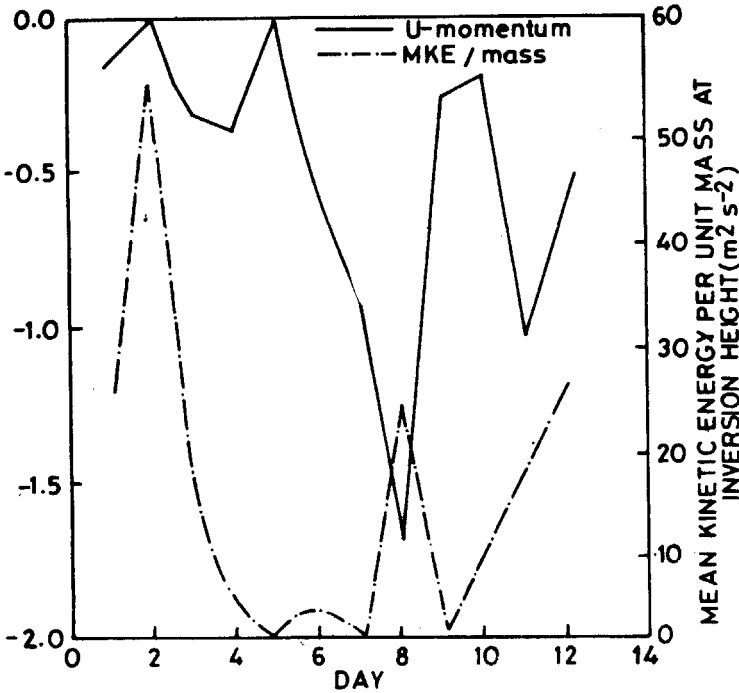


Fig 5 Day to day variation of  $U$ -momentum and  $MKE/m$  at  $Z_i$ .

spectra<sup>19</sup> and considering  $\epsilon$  not exactly constant with height within the mixed layer under stable fumigation conditions

$$\left(\frac{C_v^2}{2.2}\right) = \epsilon^{2/3} \dots (8)$$

$C_v^2$  is determined in the Kolmogorov range of turbulence by expression<sup>20</sup>

$$C_v^2 \cong \langle [\bar{v}(\bar{x} + \Delta z) - \bar{v}(\bar{x})]^2 \rangle \Delta z^{-0.67} \dots (9)$$

where  $\Delta z = 30$  metres in our case. Using vertical wind velocity difference at locations  $\bar{x}$  and  $(\bar{x} + \Delta z)$ , equation (9) is used to compute  $C_v^2$ . Bracket  $\langle \rangle$  in this equation denotes long period (ensemble) average of fluctuations in wind velocity occurring at all levels.

### Advective Flux of U-Momentum

Kinematic flux of  $w$ -momentum in the direction of mean wind is representative of  $U$ -momentum. Magnitude of this variable can be represented by product  $(\bar{w} \cdot \bar{u})$ . Fig. 5 also shows day to day variation of its magnitude over  $Z_i$ . This reveals that a non-stationary character is inherent and the flux varies almost similar to  $MKE/m$  at  $Z_i$  (shown in the right ordinate of Fig. 5). However, corresponding magnitudes start varying inversely when the pressure trough



over our observation station begins to intensify (exactly from day 7 onwards) as per ref. 10. Turbulence intensity is also found to decrease rapidly at existing inversion depth. Wind shear values given by sodar at each consecutive levels reveal that on day 7 there was a sharp increase in magnitude of  $U$ -momentum which may be due to pronounced entrainment or a sinking motion. This also signifies that free flow above  $Z_i$  and the mixed layer below exchange moisture vigorously, resulting into a sudden increase in the  $U$ -momentum<sup>21</sup>.

### Dissipation Length Scale

This scale ( $d_l$ ) is similar to mixing length in the ABL but for our studies, mostly confined to early morning inversion depths, we compute this scale by considering a direct relationship of  $\epsilon$  and the measurable vertical velocity ( $v_l$ ) as per Arya<sup>22</sup>

$$\epsilon = \frac{v_l^3}{d_l} \quad \dots (10)$$

If the flow is assumed to be isotropic i.e., wind parameter as discussed vary uniformly in all the directions, then a return-to-isotropy condition as per equations for turbulent flux terms<sup>23</sup> are assumed to be proportional to the corresponding flux divided by energy containing eddy time scale ( $\tau$ ) where<sup>22</sup>  $\tau \sim d_l/v_l$ . Now, considering sodar measured  $\sigma_w \approx d_l/\tau$  the empirical form of Hunt *et al.*<sup>24</sup> may be used

$$d_l = 0.4 \left( \frac{\sigma_w^3}{\epsilon} \right) \quad \dots (11)$$

$d_l$  is found to lie in the range between 2 and 30 metres. From Fig. 6 it is also to be noted that the scale varies almost linearly with  $Z_i$ .

### Comparison of Length Scales Occurring on Day 7 and 11

On September 7 (day 11) which is a day after the passage of the depression over station KGP, just above surface layer, streaks of dark structures were recorded on sodar facsimile (Fig. 7) in the time period between 1047 and 1200 hours, LST. This structure was frequently observed at various depths during MONTBLEX (relative occurrence was about 21% of time). Table II gives a summary of some of their morphologies. The structure so observed resembles to that of type 9 of Clark *et al.*<sup>25</sup>, Fig. 18 of Singal<sup>26</sup> and to Fig. 8 of Gaynor *et al.*<sup>27</sup>. The structure is contiguous till 1100 hours LST. Surface layer moisture show a sudden increase (see Fig. 8). The structure appears after a spell of heavy rain and is also followed by a moderate rainfall.

Day 7 (September 3), on the other hand, typically represents the period when concentration phase of Typhoon 'Becky' is almost well formed into a depression. Dense cloud was ubiquitous over the North Bay of Bengal and there was no surface pressure tendency observed on the day.

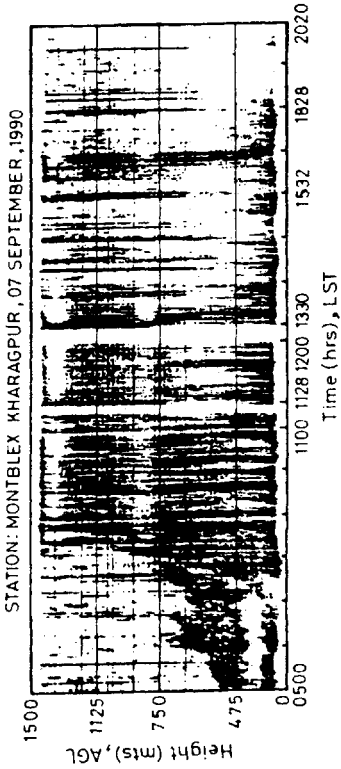


Fig 7 Sodar facsimile pertaining to ABL thermal structure observed on day 11 (during period between 0500-1100 hours LST; 1128-1200 hours LST and 1330-2020 hours LST)

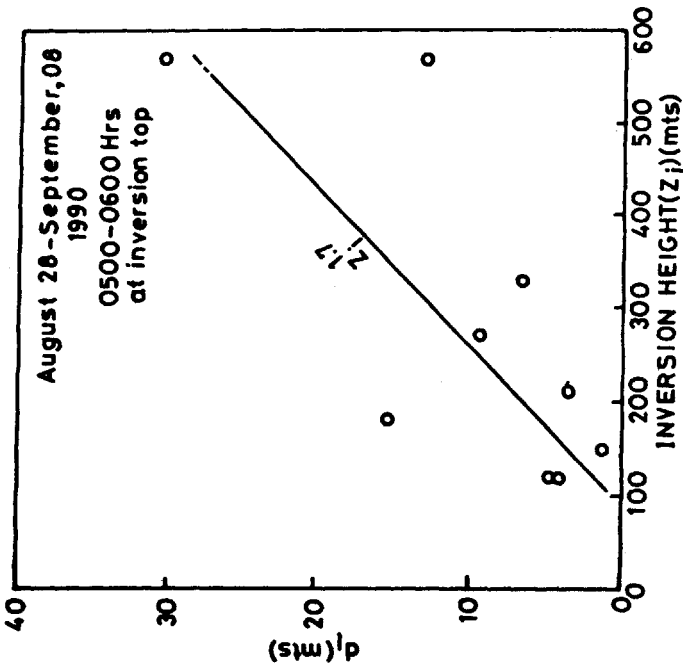


Fig 6 A regression line ( $d_i$  versus  $Z_i$ ) obtained from considering all days' data

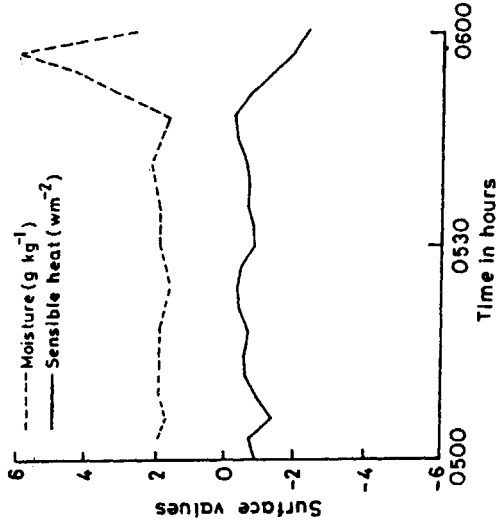


Fig 8 Surface values of humidity mixing ratio and sensible heat flux in the period between 0500-0600 hours LST on September 07, 1990

Table II

Summary of sodar structures observed during the observation period at various hours of sounding

Day	Interval (Hrs) (LST)	Structure (Depth) (mts.)	Surface Wind (m/s)	Other Echoes
1	1014-1206	750	4.8-6.2	Rising plumes
4	1306-1500	755	8.4	Rising plumes
6	0530-0715	450	0.8-1.7	Dark band (rain)
6	1200-1250	308	0.8-1.3	Dark band (rain)
7	0530-1305	600	3.5	Random dots with scarce short lived lumps
8	0530-1305	450	3.5-5.8	Lumps also visible, Rising plumes
9	1530-1630	750	4.7	Lumps also visible
11	1047-1220	600	5.7	Preceded and followed by heavy rain
12	1440-1600	200	4.8-7.1	Preceded by rain

### Kolmogorov Microscale Over $Z_i$

It is found that on September 3 (day 7) between 0500 and 0800 hours LST there is an intermittency in occurrence of height-ramped magnitudes of Kolmogorov microscales occurring in the intermediate ranges (see Fig. 9b). In the period between 0550 and 0650 hours LST this scale increases with height with a base value of  $1.8 \times 10^{-3}$  mt at a depth of about 640 metres AGL. On the contrary, on September 7 (day 11) there occurs maximum uniformity as observed in the magnitudes of these scales (cf. Figs 9b and 11). At around 1120 metres range after 0900 hours,  $\eta_k$  magnitude is about  $1.46 \times 10^{-3}$  mt and goes on decreasing further upward.

In this time between 0700 and 0800 hours LST the magnitude is almost insignificant and the surface records show rainfall activity. Above 1000 metres AGL, this scale maintains a constant value of around  $1.04 \times 10^{-3}$  mt (see Fig. 11) and subsequently decreases rapidly with height above. This may be due to sudden transition of the ABL from less stable to a free convection state.

### Dissipation Length Scale

On day 7, between 0500 and 0800 hours LST, magnitude of  $d_l$  is almost found to be negligible and is devoid of its occurrence upto a range of 420 metres AGL (Fig. 9a). On day 11 however, magnitudes of the scale are higher (i.e.  $10 < d_l \leq 90$  metres) in the range interval of 600-1500 metres extending deep into the mixed layer (cf. Figs 9a and 10). On day 7, between 0500 and 0800 hours LST, the scale almost linearly increases within a range between 450 and 1500 metres AGL (see Fig. 9a). It is also seen that with an increase in solar heating rate (after 0600 hours LST) the scale becomes delineated in its time-

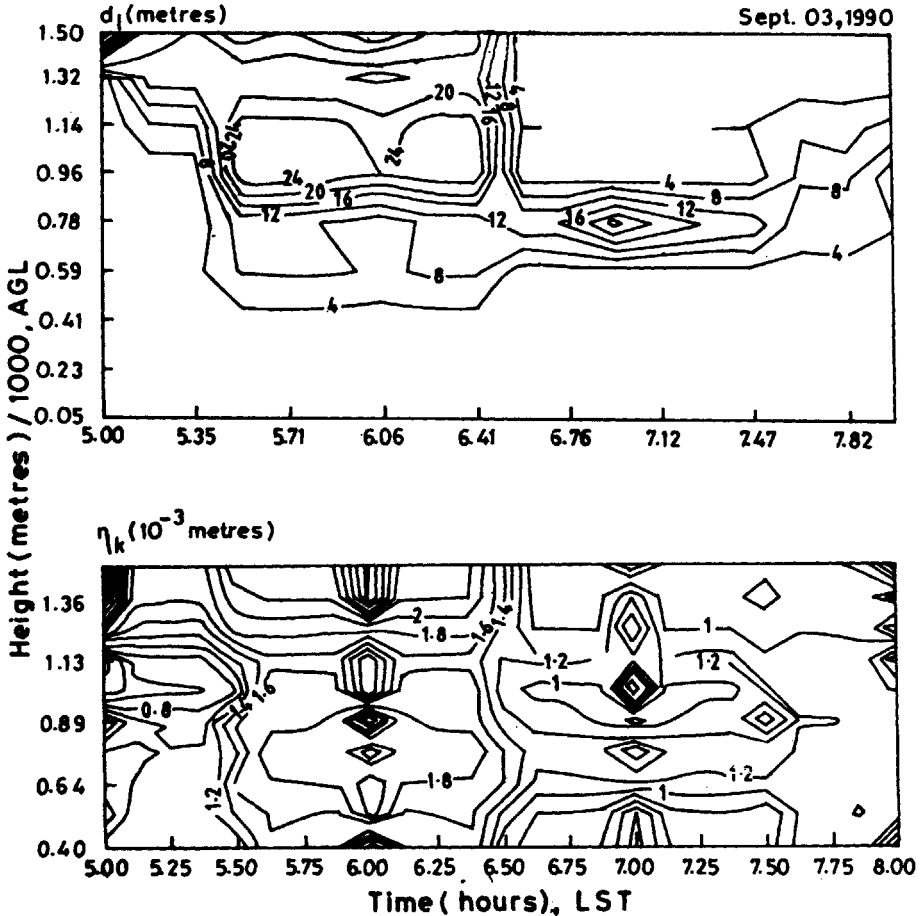


Fig 9 (a) Time-height isolines of  $d_l$ , for the period, 0500-0600 hours LST on day 7, (b) Same as in (a) but, for the Kolmogorov microscale (in mm)

height occurrence pattern. The scale also undergoes a sharp decrease with time in the levels between 780 and 1500 metres AGL.

From Doppler sodar records, it is observed that the wind-shear pertaining to this period is substantially high. While a downward vertical velocity is maintained and subsequently when free convection develops, velocity structure at that height interval becomes extremely large thereby causing  $\epsilon$  to increase. After 0700 hours LST, the scale once again reaches a maximum at a height interval between 750 and 900 metres AGL. It remains zero above 1200 metres AGL which is also the depth of a cumulus formation. It is also to be noted from Fig. 10 that its magnitude maintains a constant value in the time between 0500 and 1100 hours LST while, it becomes insignificant in the time between 1040 and 1220 hours LST. The latter period also corresponds to the occurrence of deep echoes seen as lumps on the fascimile chart, with a recurrence at around 750 metres range.

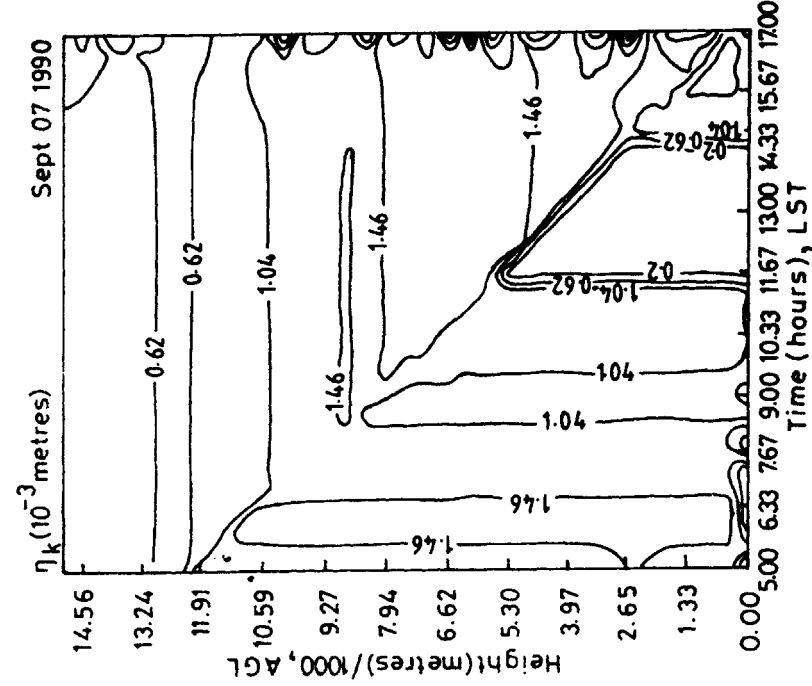


Fig 11 Same as in Fig 9(b) but, for the scales occurring in time between 0500-1700 hours LST on day 11

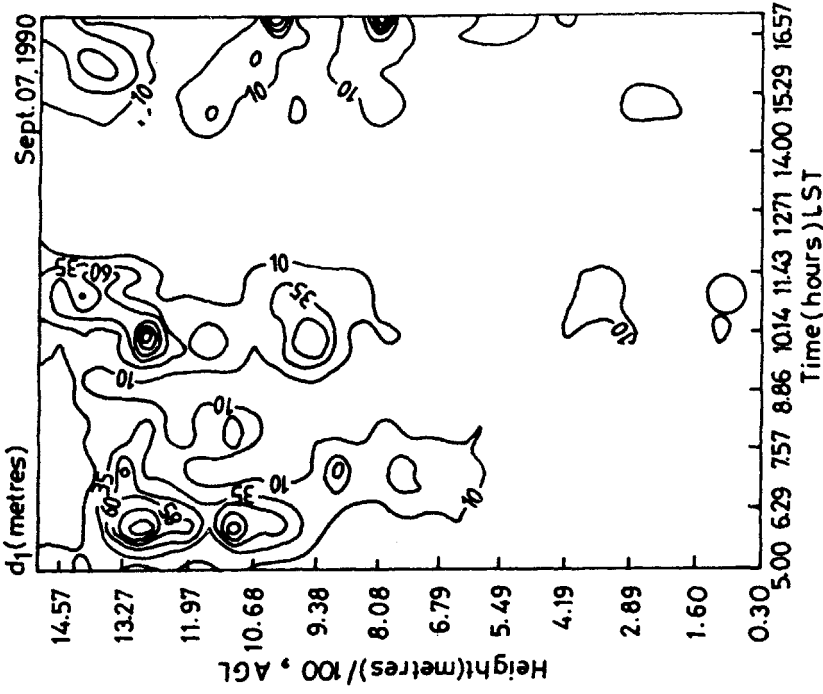


Fig 10 Same as in Fig 9(a) but, for the scales occurring in time between 0500-1700 hours LST on day 11

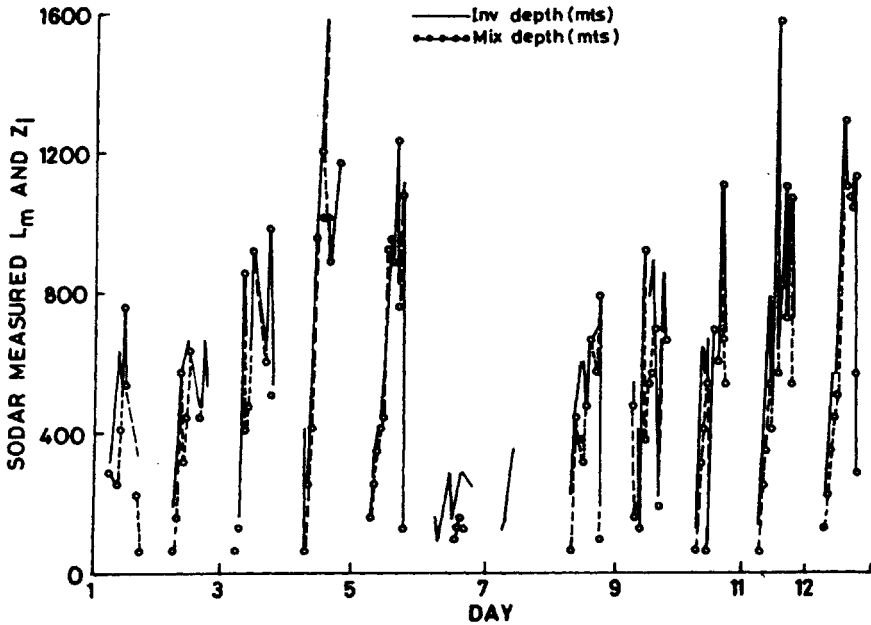


Fig 12 Diurnal variation of sodar registered  $L_m$  and  $Z_i$  magnitudes

### Summary and Conclusions

This study is based on analysis of few motion-related quantities occurring at the ABL top during the morning hours of a monsoon phase. The situation is particularly associated with the passage of a depression. Behaviour of turbulence quantities on a day-to-day basis are reasoned with pressure trough orientation in relation to the station of observation.

Inversion-top magnitudes of mean wind turbulence quantities are found to have a decreasing trend with the northward advancement of the depression that was in its dissipation stage (day 1 through 12) and with this, the trough over the station Kharagpur is also found to intensify in strength. Turbulence intensity, vertical momentum flux along the mean wind direction, MKE per unit mass and the dissipation length scales are plotted in Figs 4, 5 and 6 respectively. Conversion of MKE per unit mass to shear kinetic energy is maximum even if the ground-based inversion depth remained favourably low during pressure trough formation.

The most notable feature about the sodar measured inversion and mixing depth in this study is that both the depths become very small during day 6 and 7 (September 2 and 3 respectively). The mixing depth remains uniform over the entire day. The difference between inversion and mixing depth is also seen to be large compared to the other days (see Fig. 12). This clearly exhibits a fact that a feeble mixing layer growth takes place in the ABL during the passage of the depression. The small mixing during the morning hours which is discernible, may only be caused due to wind shear. From already analysed

height occurrences of the Kolmogorov microscale of turbulence during sounding periods of day 11 it is found that the excess sodar backscatter causing appearance of dark structures on the facsimile (as in Fig. 7) corresponds to the period when there is an embedded occurrence of the scale, i.e., between 1040 and 1220 hours LST (cf. Figs 7 and 11). The impact of passage of the depression has a significant effect on various turbulence parameters. From Fig. 3, it is evident that all wind velocity standard deviations decrease considerably on days 6 and 7. The turbulence intensity at the inversion-top show an insignificant value as found on day 7 and it is also evident that it takes on a poor value from day 6 and onwards (see Fig. 4). The  $MKE/m$  magnitudes sharply fall on days 5, 6 and 7 as seen in Fig. 5. Lastly, the passage of the depression has most pronounced effect on the inversion depth as well as on the mixing depth during days 6 and 7.

### Acknowledgements

The authors remain indebted to the Department of Science and Technology, New Delhi, for a Research grant to pursue this work. The authors also wish to thank Mr K G Vernekar, Deputy Director of the Indian Institute of Tropical Meteorology, Pune, for his generous help in obtaining the required data-sets.

### References

- 1 J C Wyngaard *Atmospheric Turbulence and Air Pollution Modelling* (Eds. FTM Nieuwstadt and H Van Dop), D Reidel, Dordrecht (1982) Ch-3, p 69
- 2 J C R Hunt *ibid*, Ch-6, p 231
- 3 E E Gossard, W D Neff, R J Zamora and J E Gaynor *Radio Sci* **19(6)** (1984) 1523-1533
- 4 E E Gossard, Russell B Chadwick, Thomas Detman and John Gaynor *Proc Ursi Comm Symp, Belgium* (1983) 413-424
- 5 J C Kaimal and J E Gaynor *Proc fifth ISARS* (Ed. S P Singal) Tata McGraw Hill New Delhi (1990) 538pp
- 6 R J Hill *Radio Sci* **13** (1978) 953-961
- 7 R G Lamb *Atmospheric Turbulence and Air Pollution Modelling* (Eds F T M Nieuwstadt and H Van Dop) D Reidel Dordrecht (1982) Ch-5, p 159
- 8 M Goel and H N Srivastava *Bull Amer Met Soc* **71** (1990) 1594-1600
- 9 D K Rakshit and M Goel *MONTBLEX—Design and Operations Plan* Department of Science and Technology New Delhi (1990) 44pp
- 10 M G Gupta *MOCC Brief Report* India Meteorological Department New Delhi (1990) 47pp
- 11 S Sivaramakrishnan, Sangeeta Saxena and K G Vernekar *Boundary Layer Met* **60(2)** (1992) 95-108
- 12 B Roy, U K De and D K Rakshit *Indian J Phys* **68(B)** No. 3 (1994) 221-229
- 13 Z Mingyu, Chen Jingnan, Li Shiming, Zhen Yueming, Su Lirong and Lu Naiping *Acta Met Sinica* **5(3)** (1991) 331-341
- 14 R L Coulter *Jappl Met* **11** (1979) 1495-1499
- 15 Aerovironment Inc *Doppler V-2000 System Technical Manual* Aero Vironment Inc Pasadena (1988) 109pp
- 16 R B Stull *Introduction to Boundary Layer Meteorology* (Ed R B Stull) Kluwer Academic Dordrecht (1988) 817-822
- 17 G E Willis and J W Deardorff *Quart J R Met Soc* **102** (1976) 817-822
- 18 J L Lumley and H A Panofsky *Structure of Atmospheric Turbulence* Interscience (1964) Ch-2, 59-96
- 19 J C Kaimal *IITM Lecture Notes* IITM Pune (1988) Ch-II 115pp

- 20 C G Little *Proc IEEE* **57(4)** (1969) 571-578
- 21 L Mahrt *J Met Soc Japan* **59** (1981) 238-241
- 22 S P Arya *Engineering Meteorology* Vol. I Elsevier Scientific Dordrecht (1982) Ch-6, 233-266
- 23 N O Jensen and N E Busch *Engineering Meteorology* Vol. I, Elsevier Scientific Dordrecht (1982) Ch-5, 179-229
- 24 J C R Hunt, J C Kaimal and J E Gaynor *Quart J Roy Met Soc* **111** (1985) 793-815
- 25 G H Clark, E Charash and E O K Bendun · *J appl Met* **106** (1977) 1365-1371
- 26 S P Singal *Encyclopaedia of Air Pollution Control Technology*, Vol. 2 (Ed N Cheremisinoff) Gulf Publishing Houston (1989) Ch-28, 1003-1062
- 27 J E Gaynor and P A Mandics *Mon Weather Rev* **106** (1978) 223-232